Spatiotemporal Thermalization and Adiabatic Cooling of Guided Light Waves

Lucas Zanaglia,[1] Josselin Garnier,[2] Iacopo Carusotto,[3] Valérie Doya,[1] Claire Michel,[1,4] and Antonio Picozzi[5]
[1]Université Côte d'Azur, CNRS, Institut de Physique de Nice, Nice, France
[2]CMAP, CNRS, Ecole Polytechnique, Institut Polytechnique de Paris, 91120 Palaiseau, France
[3]Pitaevskii BEC Center, CNR-INO and Dipartimento di Fisica, Università di Trento, I-38123 Trento, Italy
[4]Institut Universitaire de France (IUF), 1 Rue Descartes, 75005 Paris, France
[5]Université Bourgogne Europe, CNRS, Laboratoire Interdisciplinaire Carnot de Bourgogne ICB UMR 6303, 21000 Dijon, France

(Received 16 June 2025; revised 6 November 2025; accepted 14 January 2026; published 5 February 2026)

We propose and theoretically characterize three-dimensional spatiotemporal thermalization of a continuous-wave classical light beam propagating along a multimode optical waveguide. By combining a nonequilibrium kinetic approach based on the wave turbulence theory and numerical simulations of the field equations, we anticipate that thermalizing scattering events are dramatically accelerated by the combination of strong transverse confinement with the continuous nature of the temporal degrees of freedom. In connection with the blackbody catastrophe, the thermalization of the classical field in the continuous temporal direction provides a novel intrinsic mechanism for adiabatic cooling and spatial beam condensation. This process of adiabatic cooling is distinct from other mechanisms of thermalization and provides new insights into the dynamics of far-from-equilibrium closed systems and their route to thermalization.

DOI: 10.1103/mqzh-w2gh

Introduction—Fluids of light in propagating geometries are an emerging platform to study the physics of quantum gases. In contrast to the driven-dissipative dynamics of the fluid of light in cavity configurations, these systems are characterized by a conservative Hamiltonian dynamics [1–3]. In recent years, intense efforts have been devoted to the experimental observation of the 2D relaxation dynamics of monochromatic light toward a fully thermalized equilibrium state [4–6]. In this framework, special attention is being devoted to parabolic (graded-index) multimode optical fiber configurations where spatial confinement prevents beam expansion and ensures efficient nonlinear interactions. These advances were anticipated by spatial beam-cleaning experiments [7–9] and related theoretical works [10–13] and have fueled the emergence of the new field of optical thermodynamics [10,14–21].

The physics is far richer when one goes beyond the monochromatic assumption and allows for a spatiotemporal (ST) 3D dynamics. In this case, the mapping of light propagation onto a fluid of light can be rigorously formulated at the microscopic quantum level by exchanging the role of the propagation coordinate z and of the physical time t, which leads to a full quantum fluid theory of light [22]. In synergy with pioneering experiments on quantum fluctuation features [23], the study of 3D fluids of light is closely connected with the strong ongoing activity on the spatiotemporal dynamics of light beams, in particular in multimode waveguides [24,25] (multimode solitons [26], conical emission [27], instabilities [28], supercontinuum generation [7,29]).

A natural challenge [18,30,31] is then to extend optical thermodynamics concepts to the 3D case with the ambitious objective of observing full ST thermalization of light. In waveguide geometries, the 3D extension of the transverse spatial beam cleaning so far observed only in 2D for monochromatic light would open the intriguing possibility of condensation also in the spectral domain.

In this Letter, we take inspiration from ongoing efforts in the cold-atom context [32–36] to propose a strategy to observe an efficient 3D thermalization of classical waves in both the spatial and the temporal directions. While spatial confinement is guaranteed by a multimode waveguide geometry, the use of a temporally continuous incoherent input wave instead of the usual coherent pulses [4–9,14–19] guarantees that the beam remains homogeneous in the temporal direction with no need for confinement to overcome pulse broadening effects. In contrast to the extremely slow thermalization of quantum light predicted in [31], bosonic stimulation effects [37–41] are anticipated to strongly accelerate thermalization of classical waves. As a key feature of ST thermalization, we show how the presence of a continuum of temporal modes overcomes the obstacles imposed by the discrete waveguide modes onto the spatial-only thermalization [41–43]. On top of a fast convergence toward a local Rayleigh-Jeans (RJ) ST equilibrium, we anticipate an unexpected process of adiabatic cooling, which opens new perspectives on the nonequilibrium dynamics of closed systems and on their paths to thermalization [44–49].

The NLSE model—Consider a random classical field with central frequency $\tilde{\omega}_o$ propagating along the z-axis of a waveguide; see Fig. 1(a). At a simple yet accurate level of approximation, we describe the slowly varying field envelope $\psi(t,\boldsymbol{r},z)$ around the carrier frequency $\tilde{\omega}_o$ and wave vector k_o in terms of a nonlinear Schrödinger equation (NLSE) [3,22]:

$$i\partial_z\psi = -\frac{1}{2k_o}\nabla_\perp^2\psi + V(\boldsymbol{r})\psi + \kappa_2\partial_t^2\psi - \gamma_o|\psi|^2\psi. \quad (1)$$

The propagation distance z plays the role of an evolution "time" variable, while t plays the role of a spatial variable in the reference frame that propagates with group velocity $v_g^{-1} = \partial_{\tilde{\omega}}k(\tilde{\omega}_o)$. Here, $k(\tilde{\omega})$ is the dispersion relation as a function of the frequency $\tilde{\omega}$, and the carrier satisfies $k_o = k(\tilde{\omega}_o)$. The parameter $\kappa_2 = \frac{1}{2}\partial_{\tilde{\omega}}^2 k(\tilde{\omega}_o)$ denotes the dispersion coefficient, γ_o the nonlinear coefficient, and the transverse trapping potential $V(\boldsymbol{r})$ accounts for the refractive index profile in the transverse $\boldsymbol{r} = (x,y)$ directions.

We introduce a real-valued orthonormal basis $u_m(\boldsymbol{r})$, with eigenvalues β_m, solutions of the transverse waveguide problem $\beta_m u_m(\boldsymbol{r}) = [-(2k_o)^{-1}\nabla_\perp^2 + V(\boldsymbol{r})]u_m(\boldsymbol{r})$. We then expand the field $\psi(t,\boldsymbol{r},z)$ in terms of its modal amplitudes $b_m(\omega,z) = \iint dt\, d\boldsymbol{r}\,\psi(t,\boldsymbol{r},z)\exp(i\omega t)u_m(\boldsymbol{r})$, which are governed by [50]

$$i\partial_z b_m = \tilde{\beta}_m(\omega)b_m - \gamma\Gamma_m(\omega)P_m(\boldsymbol{b}), \quad (2)$$

where the linear and nonlinear dispersion relations, respectively, read $\tilde{\beta}_m(\omega) = \beta_m - \kappa_2\omega^2$ and $\Gamma_m(\omega) = 1$, with $\omega = \tilde{\omega} - \tilde{\omega}_o \ll \tilde{\omega}_o$ the frequency offset from the carrier $\tilde{\omega}_o$, and $\gamma = \gamma_o/(2\pi)^2$. The interaction among modes mediated by the optical nonlinearity is $P_m(\boldsymbol{b}) = \sum_{pqr} W_{mpqr}\int b_p(\omega_1,z)b_q^*(\omega_2,z)b_r(\omega_3,z)\delta_\omega d\omega_1 d\omega_2 d\omega_3$, where $\delta_\omega = \delta(\omega-\omega_1+\omega_2-\omega_3)$ and $W_{mpqr} = \int u_m(\boldsymbol{r})u_p(\boldsymbol{r})u_q(\boldsymbol{r})u_r(\boldsymbol{r})d\boldsymbol{r}$ accounts for the spatial overlap among the eigenmodes. In realistic configurations, the truncated potential $V(\boldsymbol{r})$ guides a finite number of modes, labeled by the indices $m,p,q,r = 0,\ldots,M-1$, where M is the total number of propagative modes supported by the waveguide. Note that β_m and W_{mpqr} do not depend on the frequency ω, because we have expanded the field on ω-independent eigenmodes $\{u_m(\boldsymbol{r})\}$ [50].

While the NLSE is able to capture the essential physics in a simple and broadly accessible form, a more accurate theory—based on the unidirectional propagation equation (UPE) [55–59]—is presented in the Supplemental Material [50]. In a waveguide geometry, the UPE for the mode amplitudes $b_m(\omega,z)$ has the form Eq. (2), and the generalized linear and nonlinear dispersion effects are described by suitable functions $\tilde{\beta}_m(\omega)$ and $\Gamma_m(\omega)$ [50].

Role of resonances in the thermalization process—Nonequilibrium light thermalization is crucially driven by interactions between modes mediated by optical nonlinearities. For relatively weak nonlinearities, the efficiency of these processes strongly relies on the presence of resonances among quartets of modes. The difference in behavior between the spatial-only case for monochromatic light and the ST case is illustrated in Fig. 1(b) for the concrete example of a step-index waveguide supporting $M = 10$ modes. In particular, we show the number of mode quadruplets $\{m,p,q,r\}$ that satisfy a quasiresonance condition $|\Delta\beta_{mpqr}|L_{\rm nl} < \delta$ in the two cases. Here, $L_{\rm nl} \simeq 1/(|\gamma_o|\bar{N})$ is the nonlinear length and $\bar{N}$ the average intensity [50].

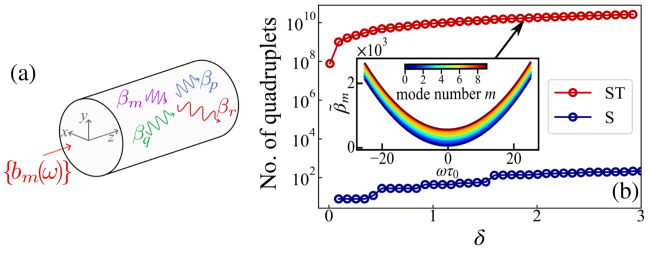

FIG. 1. Quasiresonances. (a) Schematic visualization of the waveguide. (b) Number of mode quadruplets $\{m,p,q,r\}$ verifying a resonance condition in the spatial-only $|\Delta\beta^S_{mpqr}|L_{\rm nl} < \delta$ (blue line) and in the ST $|\Delta\beta^{ST}_{mpqr}|L_{\rm nl} < \delta$ (red line) cases. The temporal degree of freedom leads to a dramatic enhancement of the number of quasiresonances. Inset: Modal dispersion relations $\tilde{\beta}_m(\omega)$ (in mm^{-1}) used to compute the resonant quadruplets in the ST case. Parameters: $L_{\rm nl} = 0.3$ m, $\tau_0 = \sqrt{|\kappa_2|L_{\rm nl}}$, $\omega_c = 25/\tau_0$ (the waveguide configuration is described in Sec. IV of Supplementary Material [50]).

In the spatial case, typically large values of the detunings $\Delta\beta^S_{mpqr} = \beta_m + \beta_q - \beta_p - \beta_r$ suppress thermalization in generic waveguides [11] unless resonances are enforced by symmetry reasons, e.g., in parabolic-shaped multimode fibers [9]. In the ST case, instead, β_m is replaced by the continuous frequency-dependent dispersion $\tilde{\beta}_m(\omega) = \beta_m - \kappa_2\omega^2$. The inset of Fig. 1(b) reports an example of $\tilde{\beta}_m(\omega)$ in the anomalous dispersion regime ($\kappa_2 < 0$). The four-mode detuning parameter now reads $\Delta\tilde{\beta}^{\omega 123}_{mpqr} = \tilde{\beta}_m(\omega) - \tilde{\beta}_p(\omega_1) + \tilde{\beta}_q(\omega_2) - \tilde{\beta}_r(\omega_3)$. The extra degree of freedom introduced by ω ensures the existence of efficient resonances $|\Delta\beta^{ST}_{mpqr}|L_{\rm nl} \ll 1$ for the different quartets of modes, where for each quartet, $\Delta\beta^{ST}_{mpqr} = \min(\Delta\tilde{\beta}^{\omega 123}_{mpqr})$ is optimized over the frequencies $\{\omega,\omega_{1,2,3}\}$ in the range $|\omega| \le \omega_c$ of our simulations. As evidenced in Fig. 1(b), the number of quasiresonances in the ST case exceeds the one in the spatial-only case by several orders of magnitude, guaranteeing efficient thermalization. This result is general and totally independent of the specific waveguide configuration considered [50].

Spatiotemporal wave turbulence—The intuitive physical picture about resonant interactions depicted in Fig. 1 can be

formalized in the framework of the wave turbulence theory, which provides a detailed nonequilibrium description of the irreversible thermalization process [30,41,43,60–66]. As anticipated in Fig. 1, in the spatial case, the transverse confinement of the field imposed by the potential $V(\boldsymbol{r})$ leads to a *discrete* set of resonant interactions, which can suppress efficient quasiresonances and ultimately freezes the thermalization process. This aspect was discussed in the context of discrete wave turbulence [41–43,67–70]. In this discrete turbulence regime, it is not possible to derive a *continuous* kinetic equation describing spatial-only thermalization (see Sec. III in Supplementary Material [50]).

Conversely, we show that the continuous nature of the temporal degrees of freedom restores efficient ST resonances, enabling the derivation of a *hybrid discrete-continuous* ST kinetic equation involving discrete sums over the spatial modes and continuous integrals over the temporal spectrum. We consider random initial conditions with statistically stationary (in time) distribution. The initial spectrum $n_m(\omega,0)$ is such that $\langle b_m(\omega,0)b_p^*(\omega',0)\rangle = n_m(\omega,0)\delta_{mp}\delta(\omega-\omega')$, where δ_{mp} is the Kronecker symbol, and the brackets $\langle\cdot\rangle$ denote an average with respect to the distribution of the random initial conditions. In the weakly nonlinear regime, we derive in the Supplemental Material [50] the kinetic equation for the evolution of the ST spectrum $n_m(\omega,z)$ such that $\langle b_m(\omega,z)b_p^*(\omega',z)\rangle = n_m(\omega,z)\delta_{mp}\delta(\omega-\omega')$:

$$\partial_z n_m(\omega,z) = 4\pi\gamma^2\sum_{pqr}\int d\omega_{1-3}|W_{mpqr}|^2\boldsymbol{M}_{mpqr}(\boldsymbol{n}) \times \delta(\omega-\omega_1+\omega_2-\omega_3)\delta(\Delta\tilde{\beta}^{\omega 123}_{mpqr}) \tag{3}$$

with the cubic nonlinear term $\boldsymbol{M}_{mpqr}(\boldsymbol{n}) = n_p(\omega_1)\times n_q(\omega_2)n_r(\omega_3) + n_m(\omega)n_p(\omega_1)n_r(\omega_3) - n_m(\omega)n_q(\omega_2)\times n_r(\omega_3) - n_m(\omega)n_p(\omega_1)n_q(\omega_2)$. Note that degenerate modes have been neglected; see Supplementary Material [50].

The kinetic equation (3) conserves the particle number $N=\sum_m[1/(2\pi)^2]\int n_m(\omega)d\omega$, the momentum $P=\sum_m[1/(2\pi)^2]\int\omega n_m(\omega)d\omega$, and the kinetic energy $E=\sum_m[1/(2\pi)^2]\int\tilde{\beta}_m(\omega)n_m(\omega)d\omega$ [71]. At the same time, it exhibits an H-theorem of entropy growth $\partial_z S(z)\geq 0$ for the nonequilibrium entropy $S(z)=\sum_m\int\log\big(n_m(\omega)\big)d\omega$: at variance with the NLSE [Eq. (2)] that is formally reversible (Hamiltonian) in time z, it then describes the actual nonequilibrium process of ST thermalization toward the RJ equilibrium:

$$n_m^{RJ}(\omega)=\frac{T}{\tilde{\beta}_m(\omega)-\lambda\omega-\mu}, \tag{4}$$

where the temperature T, chemical potential μ, and average "velocity" λ are determined from the three conserved quantities (N, P, E). Note that, in the framework of the UPE, the generalized linear and nonlinear dispersive effects enrich the form of the RJ distribution, yielding $n_m^{RJ}(\omega)=T\Gamma_m(\omega)/(\tilde{\beta}_m(\omega)-\lambda\omega-\mu)$ (Figs. 2 and 3 in Supplementary Material [50]).

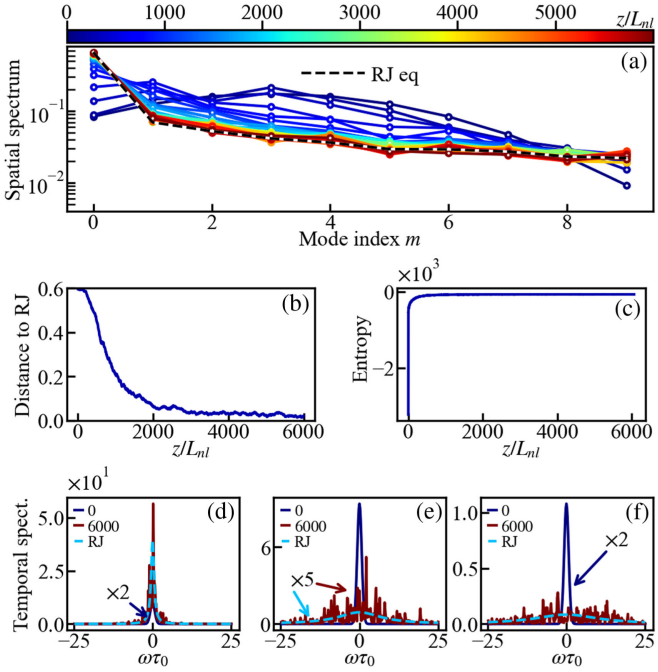

FIG. 2. Spatiotemporal thermalization. (a) Simulation of NLSE, Eq. (2). Evolution of spatial modal occupation N_m^{ST}/N, showing the relaxation to the equilibrium RJ distribution, Eq. (4) (dashed black line). (b) Evolution of the distance $\mathcal{D}^{ST}(z)$ to equilibrium, whose decrease to zero evidences ST thermalization. (c) This irreversible process is characterized by a monotonous growth of entropy, as described by the H-theorem of the wave turbulence kinetic, Eq. (3). The distance and entropy evolutions are in contrast with those of the spatial case; see Figs. 3(b) and 3(c). Temporal spectrum $|b_m(\omega,z)|^2$ of the fundamental mode $m=0$ (d), intermediate mode $m=5$ (e), highest mode ($m=9$) (f), at $z=0$ (dark blue) and $z=5000L_{\rm nl}$ (red), showing thermalization to RJ spectra (dashed light blue). Parameters: step-index waveguide supporting $M=10$ modes [see Fig. 1(b)], with anomalous dispersion and defocusing nonlinearity, $\tau_0=\sqrt{|\kappa_2|L_{\rm nl}}$, $L_{\rm nl}=0.3$ m, $\omega_c=25/\tau_0$, $\sigma_\omega=1/\tau_0$ [50].

Spatiotemporal simulations—To put these ideas on quantitative grounds, we have performed simulations of the NLSE [Eq. (2)]. The initial condition is a spatiotemporally incoherent field: the different (ω,m) components $b_m(\omega,z=0)$ are independent complex-valued Gaussian random variables of zero mean; each spatial mode m has a Gaussian spectrum $\sim\exp(-\omega^2/\sigma_\omega^2)$, with the same width $\sigma_\omega=1/\tau_0$ for all modes, and different amplitudes; see dark blue curves in Figs. 2(a) and 2(d)–2(f).

ST thermalization to the RJ equilibrium, Eq. (4), is illustrated in Fig. 2. Here, the parameters (T,λ,μ) in Eq. (4) are computed by considering the frequency cutoff $\omega_c\tau_0=25$ of the spectral grid used in the simulation [50]. In order

to compare the ST dynamics with the spatial-only dynamics (see Fig. 3 below), we report in Fig. 2(a) the evolution of the spatial mode distribution by integrating over the temporal frequencies, $N_m^{ST}(z) = [1/(2\pi)^2] \int n_m(\omega, z) d\omega$. ST thermalization is confirmed by the evolution of the distance to RJ equilibrium $\mathcal{D}^{ST}(z) = \sum_m |N_m^{ST}(z) - N_m^{RJ}| / \sum_m [N_m^{ST}(z) + N_m^{RJ}]$, with $N_m^{RJ} = [1/(2\pi)^2] \int n_m^{RJ}(\omega) d\omega$ (note that $\mathcal{D}^{ST}$ is bounded, $0 \leq \mathcal{D}^{ST} \leq 1$). As evidenced in Fig. 2(b), the distance $\mathcal{D}^{ST}(z)$ decreases to zero during propagation, while the temporal spectra converge to those predicted by the RJ equilibrium; see Figs. 2(d)–2(f). Note that, to avoid the formation of temporal solitons and the subsequent freezing of the thermalization process, a defocusing nonlinearity had to be used in the anomalous dispersion regime considered in Fig. 2. Of course, temporal solitons could be avoided also in the focusing regime by considering the normal dispersion regime.

Spatial vs spatiotemporal dynamics—To clearly evidence the key role of the temporal degrees of freedom, we compare the ST simulation in Fig. 2 with the equivalent simulation in the purely spatial problem, where the spatial modal amplitudes $b_m^S(z)$ are ruled by

$$i\partial_z b_m^S = \beta_m b_m^S - \gamma_o \sum_{p,q,r} W_{mpqr} b_p^S b_q^{S*} b_r^S. \tag{5}$$

The evolution of the spatial mode distribution $N_m^S(z) = |b_m^S(z)|^2$ is then compared to the ST evolution $N_m^{ST}(z)$, considering the same initial condition, $N_m^S(z=0) = N_m^{ST}(z=0)$. The comparison is striking: in the ST case (Fig. 2), the evolution exhibits a fast relaxation to equilibrium, whereas in the spatial case (Fig. 3), the thermalization process is frozen. This is confirmed by the evolution of the distance $\mathcal{D}^S(z) = \sum_m |N_m^S(z) - N_m^{RJ}| / \sum_m [N_m^S(z) + N_m^{RJ}]$ to the spatial RJ equilibrium $N_m^{RJ} = T^S/(\beta_m - \mu^S)$: in contrast to $\mathcal{D}^{ST}(z)$ in Fig. 2(b), $\mathcal{D}^S(z)$ does not decrease in Fig. 3(b).

Further insight on the profound distinction between the ST dynamics and the pure spatial dynamics is offered by the evolution of entropy. In the ST case, the irreversible process of thermalization is featured by a monotonic increase of entropy, as dictated by the H-theorem of entropy growth inherent to the kinetic equation (3); see Fig. 2(c). Note that the entropy growth saturates rapidly compared to the slow decrease of the distance $\mathcal{D}^{ST}$, since the latter is mainly driven by highly populated low-order modes, while the entropy is more sensitive to weakly populated high-order modes. On the other hand, the spatial dynamics shown in Fig. 3(c) evolves in a discrete wave turbulence regime governed by a *reversible* system of kinetic equations: this system does not exhibit an H-theorem of entropy growth and explains the frozen thermalization observed in Fig. 3; see Fig. 1 in Supplementary Material [50].

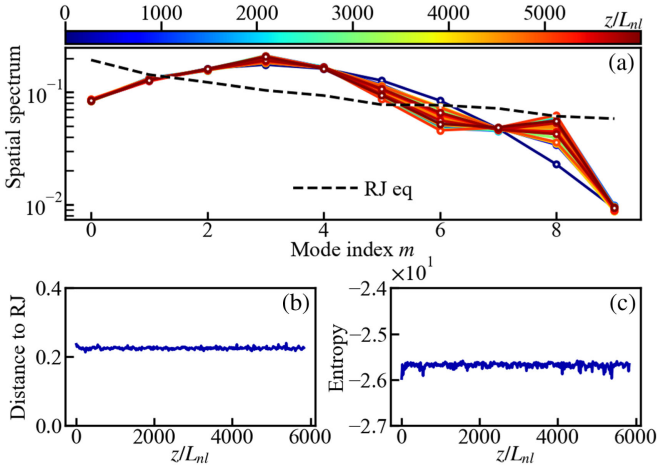

FIG. 3. Pure spatial dynamics: frozen thermalization. (a) Simulation of Eq. (5). Evolution of the spatial spectrum N_m^S/N starting from the same initial condition as in the ST simulation in Fig. 2. The thermalization process is frozen, as evidenced by the distance $\mathcal{D}^S(z)$ to RJ equilibrium (b) and the entropy (c), which, in contrast to the ST case of Figs. 2(b) and 2(c), maintain constant values at long times. Because of the large fluctuations of individual realizations, an average has been taken over 14 realizations.

Adiabatic cooling—A well-known issue of classical field theories is the occurrence of ultraviolet (UV) divergences in the thermal equilibrium state, the so-called blackbody catastrophe [39,41,60]. In our configuration, this issue is naturally tamed in the transverse direction by the finite number of modes of the waveguide, but it gives rise to a rich physics in the temporal direction. Starting from the very nonthermal initial state with a short-tailed Gaussian distribution considered in our simulations, after a transient, the optical field approaches at each z a local quasiequilibrium state that closely approximates a truncated RJ equilibrium distribution within a limited RJ window $[-\omega_c^{\rm loc}(z), \omega_c^{\rm loc}(z)]$ and quickly drops to zero outside it, as illustrated in the mode-integrated spectrum shown in Fig. 4(a). The accuracy of the process of local thermalization is evidenced by the remarkable agreement visible in Fig. 4(b) between the modal populations $N_m^{\rm loc}(z)$ predicted by the local RJ equilibrium (circles) and the ones $N_m^{ST}(z)$ computed from the NLSE simulation (solid lines).

For increasing z, the bounded window $[-\omega_c^{\rm loc}(z), \omega_c^{\rm loc}(z)]$ of the local RJ equilibrium expands, as shown in Fig. 4(c). Correspondingly, the local thermodynamic parameters also display a marked z dependence, as expected by imposing conservation of (N, P, E) in the presence of the z-dependent truncation at $\omega_c^{\rm loc}(z)$. The local temperature $T^{\rm loc}(z)$ plotted in Fig. 4(d) displays a monotonic decrease due to the continuous transfer (at a constant energy $E = \text{const}$) of the incoherent beam fluctuations into the high-energy tails of the spectrum distribution. The detailed evolution of $\omega_c^{\rm loc}(z)$ and $T^{\rm loc}(z)$ depend on all physical parameters γ, κ_2,

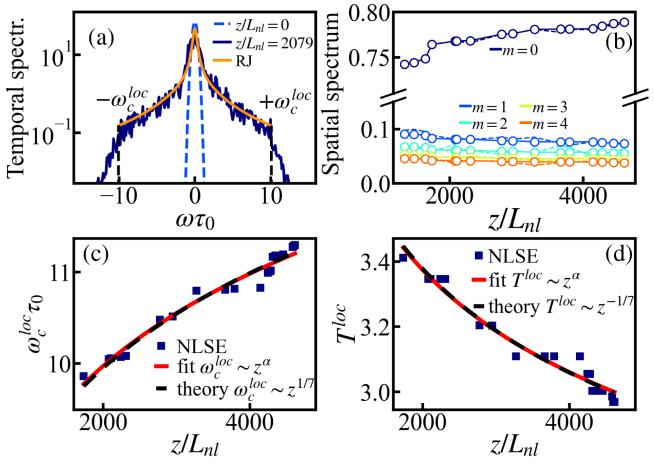

FIG. 4. Local-equilibrium route to ST thermalization and adiabatic cooling. (a) Mode-integrated temporal spectrum of the field $\sum_m |b_m(\omega,z)|^2$ at $z=0$ (light blue), $z=2079L_{\rm nl}$ (dark blue), and local RJ equilibrium distribution over the reduced frequency window $[-\omega_c^{\rm loc}(z),\omega_c^{\rm loc}(z)]$ (orange). (b) Modal population $N_m^{\rm loc}/N$ computed from the local RJ equilibrium (circles) and modal population N_m^{ST}/N in NLSE simulation (solid lines). Corresponding evolutions during propagation of local frequency cutoff $\omega_c^{\rm loc}(z)$ (c) and local temperature $T^{\rm loc}(z)$ (d). Results of NLSE simulations (squares) are fitted by a power law $\sim z^{\alpha}$ (red lines), showing quantitative agreement with the theory in Eq. (6) (dashed black lines). The decrease in $T^{\rm loc}(z)$ reflects an adiabatic cooling, which drives a spatial beam condensation characterized by the growth of $N_0^{\rm loc}(z)/N$ in (b). Parameters: step-index waveguide supporting $M=5$ modes, with anomalous dispersion and defocusing nonlinearity, $L_{\rm nl}=0.06$ m, $\omega_c=25/\tau_0$, $\sigma_\omega=0.4/\tau_0$.

and W_{mpqs} that appear in the kinetic equation (3). It is possible, however, to derive from Eq. (3) the following theoretical scaling law that relates $\omega_c^{\rm loc}(z)$ and $T^{\rm loc}(z)$ to the propagation distance z and that is valid when $z\gg L_{\rm nl}$ (Sec. V in Supplementary Material [50]):

$$T^{\rm loc}(z)\sim 1/\omega_c^{\rm loc}(z)\sim 1/z^{1/7}. \tag{6}$$

As illustrated in Figs. 4(c) and 4(d), this power-law behavior is confirmed by NLSE simulations, whose results are fitted by power laws $\sim z^{\alpha}$, with exponents $\alpha=0.141$ for $\omega_c^{\rm loc}(z)$ and $\alpha=-0.139$ for $T^{\rm loc}(z)$, in remarkable agreement with the value $1/7\sim 0.143$ in Eq. (6). Note that, to better highlight the asymptotic behavior of Eq. (6) in Fig. 4, the nonlinear strength was increased, while the number of modes and the initial spectral widths were reduced with respect to Fig. 2—we checked that all our predictions on the adiabatic cooling are physical and do not depend on the numerical spectral grid [50].

As a direct consequence of this *conservative adiabatic cooling*, a marked beam cleaning is visible in Fig. 4(b) together with a transverse condensation effect where the population gets macroscopically concentrated in the fundamental waveguide mode, $N_0^{ST}\gg N_{m\neq 0}^{ST}$. Most interestingly, while in the numerical simulations shown in this Letter the efficiency of the cooling process is artificially limited by the numerical cutoff (ω_c) imposed by the simulation [50], in a real physical system the UV-divergent value of the energy stored in the tails of the classical distribution would, in principle, allow for an arbitrary large decrease of $T^{\rm loc}(z)$. This conclusion, however, holds only within the validity range of our classical, conservative model equation, which neglects material absorption or higher-order dissipative nonlinearities. In addition, at large frequencies the classical model ultimately breaks down as quantum statistical effects become relevant and drive the spectrum toward a Bose-Einstein distribution [31,37,39], thereby imposing an ultimate limitation to adiabatic cooling. We anyway anticipate that, given the small value of typical nonlinear media, this is expected to occur at extremely large propagation lengths z [31].

Conclusions and outlook—We developed a general wave turbulence framework for ST thermalization of light waves in multimode Kerr waveguides. For the sake of clarity, the theory and simulations presented in the main text are carried out within an NLSE formalism, but they are extended to more general and accurate UPE [Eq. (2)] in the Supplemental Material [50]. In contrast to the frozen spatial thermalization of monochromatic light, we find that the presence of the continuous temporal degrees enable efficient ST thermalization. As a consequence of the blackbody catastrophe of classical fields, our route to ST thermalization unveils an intrinsic adiabatic cooling mechanism, whereby the field fluctuations are transferred to high-frequency components along the time dimension, enabling a virtually unlimited spatial beam-cleaning condensation. This adiabatic cooling is inherently conservative, and therefore, is to be contrasted with conventional evaporative cooling techniques in Bose-Einstein condensates and with the self-similar processes of (pre-)thermalization [44–49]. As such, it provides valuable insight into the nonequilibrium dynamics of Hamiltonian systems and their pathways to thermalization. More broadly, our conservative wave-guided light configuration could enable full 3D condensation in the quantum regime, opening new avenues for ST beam cleaning and coherent light generation.

Acknowledgments—Funding was provided by Agence Nationale de la Recherche (Grants No. ANR-23-CE30-0021, No. ANR-21-ESRE-0040). Calculations were performed using HPC resources from Université Côte d'Azur's Center Azzura and DNUM-CCUB (Université de Bourgogne Europe). I. C. acknowledges financial support from the PE0000023-NQSTI project by the Italian Ministry of University and Research, cofunded by the European Union—NextGeneration EU, and from Provincia Autonoma di Trento (PAT), partly via the Q@TN initiative. I. C.'s research was supported in part by the International

Centre for Theoretical Sciences (ICTS) for participating in the program: Turbulence and vortex dynamics in 2D quantum fluids (code: ICTS/QUFLU2024/2). The authors acknowledge S. Wabnitz, M. Ferraro, T. Torres, P. E. Larré, B. Kibler, and P. Béjot for valuable discussions.

Data availability—The data that support the findings of this article are not publicly available. The data are available from the authors upon reasonable request.

[1] I. Carusotto, Quantum fluids of light, in *Encyclopedia of Condensed Matter Physics*, 2nd ed. (2024), 10.1016/B978-0-323-90800-9.00172-4.

[2] J. Bloch, I. Carusotto, and M. Wouters, Nonequilibrium Bose–Einstein condensation in photonic systems, Nat. Phys. Rev. **4**, 470 (2022).

[3] Q. Glorieux, C. Piekarski, Q. Schibler, T. Aladjidi, and M. Baker-Rasooli, Paraxial fluids of light, Adv. At. Mol. Opt. Phys. **74**, 157 (2025).

[4] K. Baudin, A. Fusaro, K. Krupa, J. Garnier, S. Rica, G. Millot, and A. Picozzi, Classical Rayleigh-Jeans condensation of light waves: Observation and thermodynamic characterization, Phys. Rev. Lett. **125**, 244101 (2020).

[5] H. Pourbeyram, P. Sidorenko, F. Wu, L. Wright, D. Christodoulides, and F. Wise, Direct observations of thermalization to a Rayleigh–Jeans distribution in multimode optical fibres, Nat. Phys. **18**, 685 (2022).

[6] F. Mangini, M. Gervaziev, M. Ferraro, D. S. Kharenko, M. Zitelli, Y. Sun, V. Couderc, E. V. Podivilov, S. A. Babin, and S. Wabnitz, Statistical mechanics of beam self-cleaning in GRIN multimode optical fibers, Opt. Express **30**, 10850 (2022).

[7] L. G. Wright, Z. Liu, D. A. Nolan, M.-J. Li, D. N. Christodoulides, and F. W. Wise, Self-organized instability in graded-index multimode fibres, Nat. Photonics **10**, 771 (2016).

[8] K. Krupa, A. Tonello, B. M. Shalaby, M. Fabert, A. Barthélémy, G. Millot, S. Wabnitz, and V. Couderc, Spatial beam self-cleaning in multimode fibres, Nat. Photonics **11**, 237 (2017).

[9] For a review, see M. Ferraro, F. Mangini, M. Zitelli, and S. Wabnitz, On spatial beam self-cleaning from the perspective of optical wave thermalization in multimode graded-index fibers, Adv. Phys. X **8**, 2228018 (2023).

[10] F. O. Wu, A. U. Hassan, and D. N. Christodoulides, Thermodynamic theory of highly multimoded nonlinear optical systems, Nat. Photonics **13**, 776 (2019).

[11] J. Garnier, A. Fusaro, K. Baudin, C. Michel, K. Krupa, G. Millot, and A. Picozzi, Wave condensation with weak disorder versus beam self-cleaning in multimode fibers, Phys. Rev. A **100**, 053835 (2019).

[12] A. Ramos, L. Fernández-Alcázar, T. Kottos, and B. Shapiro, Optical phase transitions in photonic networks: A spin-system formulation, Phys. Rev. X **10**, 031024 (2020).

[13] F. O. Wu, Q. Zhong, H. Ren, P. S. Jung, K. G. Makris, and D. N. Christodoulides, Thermalization of light's orbital angular momentum in nonlinear multimode waveguide systems, Phys. Rev. Lett. **128**, 123901 (2022).

[14] K. Baudin, J. Garnier, A. Fusaro, N. Berti, C. Michel, K. Krupa, G. Millot, and A. Picozzi, Observation of light thermalization to negative temperature Rayleigh-Jeans equilibrium states in multimode optical fibers, Phys. Rev. Lett. **130**, 063801 (2023).

[15] M. Ferraro, F. Mangini, K. Stefánska, W. A. Gemechu, F. Frezza, V. Couderc, M. Gervaziev, D. Kharenko, S. Babin, and S. Wabnitz, Negative absolute temperature attractor in a dense photon gas, arXiv:2505.21163.

[16] M. Ferraro, F. Mangini, F. O. Wu, M. Zitelli, D. N. Christodoulides, and S. Wabnitz, Calorimetry of photon gases in nonlinear multimode optical fibers, Phys. Rev. X **14**, 021020 (2024).

[17] M. S. Kirsch, G. G. Pyrialakos, R. Altenkirch, M. A. Selim, J. Beck, T. A. W. Wolterink, H. Ren, P. S. Jung, M. Khajavikhan, A. Szameit, M. Heinrich, and D. N. Christodoulides, Observation of Joule–Thomson photon-gas expansion, Nat. Phys. **21**, 214 (2025).

[18] E. V. Podivilov, F. Mangini, O. S. Sidelnikov, M. Ferraro, M. Gervaziev, D. S. Kharenko, M. Zitelli, M. P. Fedoruk, S. A. Babin, and S. Wabnitz, Thermalization of orbital angular momentum beams in multimode optical fibers, Phys. Rev. Lett. **128**, 243901 (2022).

[19] N. Berti, K. Baudin, A. Fusaro, G. Millot, A. Picozzi, and J. Garnier, Interplay of thermalization and strong disorder: Wave turbulence theory, numerical simulations, and experiments in multimode optical fibers, Phys. Rev. Lett. **129**, 063901 (2022).

[20] M. Lian, Y. Geng, Y.-J. Chen, Y. Chen, and J.-T. Lü, Coupled thermal and power transport of optical waveguide arrays: Photonic Wiedemann-Franz law and rectification effect, Phys. Rev. Lett. **133**, 116303 (2024).

[21] A. Kurnosov, L. J. Fernández-Alcázar, A. Ramos, B. Shapiro, and T. Kottos, Optical kinetic theory of nonlinear multimode photonic networks, Phys. Rev. Lett. **132**, 193802 (2024).

[22] P.-E. Larré and I. Carusotto, Propagation of a quantum fluid of light in a cavityless nonlinear optical medium: General theory and response to quantum quenches, Phys. Rev. A **92**, 043802 (2015).

[23] J. Steinhauer, M. Abuzarli, T. Aladjidi, T. Bienaimé, C. Piekarski, W. Liu, E. Giacobino, A. Bramati, and Q. Glorieux, Analogue cosmological particle creation in an ultracold quantum fluid of light, Nat. Commun. **13**, 2890 (2022).

[24] G. Agrawal, *Nonlinear Fiber Optics*, 6th ed. (Academic, New York, 2019).

[25] L. G. Wright, F. O. Wu, D. N. Christodoulides, and F. W. Wise, Physics of highly multimode nonlinear optical systems, Nat. Phys. **18**, 1018 (2022).

[26] Y. Sun, P. Parra-Rivas, G. P. Agrawal, T. Hansson, C. Antonelli, A. Mecozzi, F. Mangini, and S. Wabnitz, Multimode solitons in optical fibers: A review, Photonics Res. **12**, 2581 (2024).

[27] B. Kibler and P. Béjot, Discretized conical waves in multimode optical fibers, Phys. Rev. Lett. **126**, 023902 (2021).

[28] K. Krupa, A. Tonello, A. Barthélémy, V. Couderc, B. M. Shalaby, A. Bendahmane, G. Millot, and S. Wabnitz, Observation of geometric parametric instability induced

by the periodic spatial self-imaging of multimode waves, Phys. Rev. Lett. **116**, 183901 (2016).
[29] Z. Eslami, L. Salmela, A. Filipkowski, D. Pysz, M. Klimczak, R. Buczynski, J. M. Dudley, and G. Genty, Two octave supercontinuum generation in a non-silica graded-index multimode fiber, Nat. Commun. **13**, 2126 (2022).
[30] A. Picozzi, J. Garnier, T. Hansson, P. Suret, S. Randoux, G. Millot, and D. N. Christodoulides, Optical wave turbulence: Toward a unified nonequilibrium thermodynamic formulation of statistical nonlinear optics, Phys. Rep. **542**, 1 (2014).
[31] A. Chiocchetta, P. E. Larré, and I. Carusotto, Thermalization and Bose-Einstein condensation of quantum light in bulk nonlinear media, Europhys. Lett. **115**, 24002 (2016).
[32] Y. Castin, R. Dum, E. Mandonnet, A. Minguzzi, and I. Carusotto, Coherence properties of a continuous atom laser, J. Mod. Opt. **47**, 2671 (2000).
[33] E. Mandonnet, A. Minguzzi, R. Dum, I. Carusotto, Y. Castin, and J. Dalibard, Evaporative cooling of an atomic beam, Eur. Phys. J. D **10**, 9 (2000).
[34] T. Lahaye, Z. Wang, G. Reinaudi, S. P. Rath, J. Dalibard, and D. Guéry-Odelin, Evaporative cooling of a guided rubidium atomic beam, Phys. Rev. A **72**, 033411 (2005).
[35] S. E. Olson, R. R. Mhaskar, and G. Raithel, Continuous propagation and energy filtering of a cold atomic beam in a long high-gradient magnetic atom guide, Phys. Rev. A **73**, 033622 (2006).
[36] C.-C. Chen, S. Bennetts, R. G. Escudero, B. Pasquiou, and F. Schreck, Continuous guided strontium beam with high phase-space density, Phys. Rev. Appl. **12**, 044014 (2019).
[37] M. J. Davis, S. A. Morgan, and K. Burnett, Simulations of Bose fields at finite temperature, Phys. Rev. Lett. **87**, 160402 (2001).
[38] C. Connaughton, C. Josserand, A. Picozzi, Y. Pomeau, and S. Rica, Condensation of classical nonlinear waves, Phys. Rev. Lett. **95**, 263901 (2005).
[39] P. B. Blakie, A. S. Bradley, M. J. Davis, R. J. Ballagh, and C. W. Gardiner, Dynamics and statistical mechanics of ultracold Bose gases using c-field techniques, Adv. Phys. **57**, 363 (2008).
[40] G. Krstulovic and M. Brachet, Energy cascade with small-scale thermalization, counterflow metastability, and anomalous velocity of vortex rings in Fourier truncated Gross-Pitaevskii equation, Phys. Rev. E **83**, 066311 (2011).
[41] S. Nazarenko, *Wave Turbulence*, Lectures Notes in Physics (Springer, New York, 2011).
[42] V. S. L'vov and S. V. Nazarenko, Discrete and mesoscopic regimes of finite-size wave turbulence, Phys. Rev. E **82**, 056322 (2010).
[43] M. Onorato, Y. V. Lvov, G. Dematteis, and S. Chibbaro, Wave turbulence and thermalization in one-dimensional chains, Phys. Rep. **1040**, 1 (2023).
[44] Y. Zhu, B. Semisalov, G. Krstulovic, and S. Nazarenko, Self-similar evolution of wave turbulence in Gross-Pitaevskii system, Phys. Rev. E **108**, 064207 (2023).
[45] For a review, see A. N. Mikheev, I. Siovitz, and T. Gasenzer, Universal dynamics and non-thermal fixed points in quantum fluids far from equilibrium, Eur. Phys. J. Special Topics **232**, 3393 (2023).
[46] S. Erne, R. Bücker, T. Gasenzer, J. Berges, and J. Schmiedmayer, Universal dynamics in an isolated one-dimensional Bose gas far from equilibrium, Nature (London) **563**, 225 (2018).
[47] M. Prüfer, P. Kunkel, H. Strobel, S. Lannig, D. Linnemann, C.-M. Schmied, J. Berges, T. Gasenzer, and M. K. Oberthaler, Observation of universal dynamics in a spinor Bose gas far from equilibrium, Nature (London) **563**, 217 (2018).
[48] M. A. Moreno-Armijos, A. R. Fritsch, A. D. García-Orozco, S. Sab, G. Telles, Y. Zhu, L. Madeira, S. Nazarenko, V. I. Yukalov, and V. S. Bagnato, Observation of relaxation stages in a nonequilibrium closed quantum system: Decaying turbulence in a trapped superfluid, Phys. Rev. Lett. **134**, 023401 (2025).
[49] M. Gazo, A. Karailiev, T. Satoor, C. Eigen, M. Galka, and Z. Hadzibabic, Universal coarsening in a homogeneous two-dimensional Bose gas, Science **389**, 802 (2025).
[50] See Supplemental Material at http://link.aps.org/supplemental/10.1103/mqzh-w2gh for the derivations of the general form of the UPE [Eq. (2)], the wave turbulence kinetic [Eq. (3)], and the power-law scaling [Eq. (6)]; the kinetic theory explaining the frozen thermalization in the spatial-only case (Fig. 3); and details about the numerical simulations. The Supplemental Material includes Refs. [51–54].
[51] M. Kolesik and J. V. Moloney, Nonlinear optical pulse propagation simulation: From Maxwell's to unidirectional equations, Phys. Rev. E **70**, 036604 (2004).
[52] A. Biasi, O. Evnin, and B. A. Malomed, Fermi-Pasta-Ulam phenomena and persistent breathers in the harmonic trap, Phys. Rev. E **104**, 034210 (2021).
[53] A. Fusaro, J. Garnier, K. Krupa, G. Millot, and A. Picozzi, Dramatic acceleration of wave condensation mediated by disorder in multimode fibers, Phys. Rev. Lett. **122**, 123902 (2019).
[54] E. Podivilov, D. Kharenko, V. Gonta, K. Krupa, O. S. Sidelnikov, S. Turitsyn, M. P. Fedoruk, S. A. Babin, and S. Wabnitz, Hydrodynamic 2D turbulence and spatial beam condensation in multimode optical fibers, Phys. Rev. Lett. **122**, 103902 (2019).
[55] M. Kolesik, J. V. Moloney, and M. Mlejnek, Unidirectional optical pulse propagation equation, Phys. Rev. Lett. **89**, 283902 (2002).
[56] A. Couairon and A. Mysyrowicz, Femtosecond filamentation in transparent media, Phys. Rep. **441**, 47 (2007).
[57] A. Couairon, E. Brambilla, T. Corti, D. Majus, O. de J. Ramirez-Gongora, and M. Kolesik, Practitioner's guide to laser pulse propagation models and simulation, Eur. Phys. J. Special Topics **199**, 5 (2011).
[58] A. D. Bandrauk, E. Lorin, and J. V. Moloney, *Laser Filamentation, Mathematical Methods and Models* (Springer, New York, 2016).
[59] P. Béjot, Multimodal unidirectional pulse propagation equation, Phys. Rev. E **99**, 032217 (2019).
[60] V. E. Zakharov, V. S. L'vov, and G. Falkovich, *Kolmogorov Spectra of Turbulence I* (Springer, Berlin, 1992).
[61] A. C. Newell, S. Nazarenko, and L. Biven, Wave turbulence and intermittency, Physica (Amsterdam) **152D**, 520 (2001).

[62] A. C. Newell and B. Rumpf, Wave turbulence, Annu. Rev. Fluid Mech. **43**, 59 (2011).
[63] S. K. Turitsyn, S. A. Babin, E. G. Turitsyna, G. E. Falkovich, E. Podivilov, and D. Churkin, Optical wave turbulence, in *Advances in Wave Turbulence*, World Scientific Series on Nonlinear Science Series A Vol. 83, edited by V. I. Shrira and S. Nazarenko (World Scientific, Singapore, 2013).
[64] S. A. Babin, D. V. Churkin, A. E. Ismagulov, S. I. Kablukov, and E. V. Podivilov, Four-wave-mixing-induced turbulent spectral broadening in a long Raman fiber laser, J. Opt. Soc. Am. B **24**, 1729 (2007).
[65] D. Churkin, I. Kolokolov, E. Podivilov, I. Vatnik, S. Vergeles, I. Terekhov, V. Lebedev, G. Falkovich, M. Nikulin, S. Babin, and S. K. Turitsyn, Wave kinetics of a random fibre laser, Nat. Commun. **2**, 6214 (2015).
[66] J. Laurie, U. Bortolozzo, S. Nazarenko, and S. Residori, One-dimensional optical wave turbulence: Experiment and theory, Phys. Rep. **514**, 121 (2012).
[67] Z. Wang, W. Fu, Y. Zhang, and H. Zhao, Wave-turbulence origin of the instability of Anderson localization against many-body interactions, Phys. Rev. Lett. **124**, 186401 (2020).
[68] N. Cherroret, T. Scoquart, and D. Delande, Coherent multiple scattering of out-of-equilibrium interacting Bose gases, Ann. Phys. (Amsterdam) **435**, 168543 (2021).
[69] A. Y. Ramos, C. Shi, L. J. Fernandez-Alcazar, D. N. Christodoulides, and T. Kottos, Theory of localization-hindered thermalization in nonlinear multimode photonics, Commun. Phys. **6**, 189 (2023).
[70] K. M. Frahm and D. L. Shepelyansky, Nonlinear perturbation of random matrix theory, Phys. Rev. Lett. **131**, 077201 (2023).
[71] Note that the factor $1/(2\pi)^2$ comes from the definition of the particle number for a statistically stationary in time field solution of the NLSE, $N = \int \langle |\psi(t, \boldsymbol{r}, z)|^2 \rangle d\boldsymbol{r}$.